Carbohydrate Polymers 110 (2014) 62–69

Contents lists available at ScienceDirect

Carbohydrate Polymers

journal homepage: www.elsevier.com/locate/carbpol

A novel thermo-sensitive hydrogel based on thiolated chitosan/hydroxyapatite/beta-glycerophosphate

Xujie Liu[a,1], Yan Chen[b,1], Qianli Huang[a], Wei He[a], Qingling Feng[c,*], Bo Yu[d,**]

[a] State Key Laboratory of New Ceramics and Fine Processing, School of Materials Science and Engineering, Tsinghua University, Beijing 100084, China
[b] Department of Ultrasonic Diagnosis, Zhujiang Hospital of Southern Medical University, Guangzhou 510282, China
[c] Key Laboratory of Advanced Materials (MOE), School of Materials Science and Engineering, Tsinghua University, Beijing 100084, China
[d] Department of Orthopedics, Zhujiang Hospital of Southern Medical University, Guangzhou 510282, China

ARTICLE INFO

Article history:
Received 21 February 2013
Received in revised form 16 February 2014
Accepted 20 March 2014
Available online 3 April 2014

Keywords:
Thiolated chitosan
Thermo-sensitive hydrogel
Degradation
Protein release
Cytotoxicity

ABSTRACT

In order to get a water-soluble *in situ* gel-forming system, a thiolated chitosan, chitosan-4-thiobutylamidine (CS-TBA) conjugate was synthesized and used to replace the unmodified chitosan in the application of the *in situ* gel-forming system. A novel thermo-sensitive hydrogel was prepared based on CS-TBA/hydroxyapatite (HA)/beta-glycerophosphate disodium (β-GP). The gel formation, rheological properties, morphology, degradation, cytotoxicity, as well as protein release process of the novel gel system were investigated in this study. The CS-TBA/HA/β-GP gel showed a higher storage modulus (G') and loss modulus (G'') and a decreased bovine serum albumin (BSA) release rate which was maintained the protein release for a longer time compared with the unmodified chitosan (CS)/HA/β-GP gel, due to the existence of thiol groups and/or disulfide bonds. The CS-TBA/HA/β-GP gel has a porous structure with a uniform distribution of nano-hydroxyapatite, an appropriate degradation rate and low cytotoxicity, showing potential applications in drug delivery and tissue engineering.

1. Introduction

Chitosan is a natural, cationic amino polysaccharide copolymer, the linear and partly acetylated (1–4)-2-amino-2-deoxy-β-D-glucan, is obtained by the alkaline deacetylation of chitin (Hashemi, Mirzadeh, Imani, & Samadi, 2013; Kafedjiiski, Krauland, Hoffer, & Bernkop-Schnuech, 2005). Because of its favorable biological properties such as biodegradability, biocompatibility and non-toxicity (Felt, Buri, & Gurny, 1998), chitosan has been widely used in drug delivery system and tissue engineering. Chitosan has been used in different forms such as microspheres for drug or cytokine delivery (Guerrero, Teijón, Muñiz, Teijón, & Blanco, 2010; Niu, Feng, Wang, Guo, & Zheng, 2009), scaffolds or hydrogels for cartilage, cardiac or bone tissue engineering (Chi, Yang, Chung, Chou, & Wang, 2013; Frohbergh et al., 2012; Tan, Chu, Payne, & Marra, 2009).

Among all of these forms, the hydrogel, especially the thermo-sensitive hydrogel has attracted much attention because it can be applied as an injectable material for irregular-shaped tissue repair. Chitosan, combined with β-glycerophosphate disodium (β-GP), is an outstanding *in situ* gel-forming system, which was first reported by Chenite et al. (2000). This system is available at a physiologically acceptable pH and is liquid at room temperature. When the temperature is raised to 37 °C, the physiological temperature, it can transform into a gel (Chenite, Buschmann, Wang, CHAut, & Kandani, 2001; Khodaverdi, Tafaghodi, Ganji, Abnoos, & Naghizadeh, 2012). Because of its good performance in gel-forming, this system has been successfully applied in the construction of injectable scaffolds for tissue engineering (Cho et al., 2008; Kwon et al., 2012).

The modification of chitosan has been widely studied in order to get certain additional advantageous properties (Sarti & Bernkop-Schnuerch, 2011). The amino groups are target moieties for the modification of chitosan. The reported modified chitosan includes carboxymethyl chitosan (CMC) (Chen & Park, 2003), trimethyl chitosan (TMC) (Kean, Roth, & Thanou, 2005), polyethylene glycol (PEG)-grafted chitosan (Kim et al., 2007) and polyethyleneimine (PEI) grafted-chitosan (Wong et al., 2006). The addition of thiol groups on the primary amino groups of chitosan, resulting thiolated chitosan, can improve some properties of chitosan (Kafedjiiski et al., 2005). Different from unmodified chitosan, which can only be dissolved in acid medium, the thiolated chitosan has good solubility at neutral pH. Moreover, the immobilized thiol groups are able to

* Corresponding author. Tel.: +86 10 62782770; fax: +86 10 62771160.
** Corresponding author. Tel.: +86 20 61643114.
E-mail addresses: biomater@mail.tsinghua.edu.cn (Q. Feng), gzyubo@163.com (B. Yu).
[1] These authors contributed equally to this work.

http://dx.doi.org/10.1016/j.carbpol.2014.03.065
0144-8617/

form disulfide bonds with other thiol groups in proteins, resulting in the improvement of mucoadhesion (Matsuda, Kobayashi, Itoh, Kataoka, & Tanaka, 2005). Thiolated chitosan is widely used to form hydrogels based on the formation of disulfide bonds. This is a time-dependent process. There are very few studies in which the thiolated chitosan is combined with β-GP to form a thermo-sensitive gel system. This novel system is water soluble and has some good rheological and protein release properties due to the presence of thiol groups.

In this study, a kind of thiolated chitosan, chitosan-4-thio-butylamidine (CS-TBA) conjugate was used to replace chitosan in *in situ* gel-forming system. In contrast to unmodified chitosan, CS-TBA is water soluble. A novel thermo-sensitive hydrogel was prepared based on CS-TBA/β-GP and hydroxyapatite (HA). The gelation, rheological properties, morphology, degradation, cytotoxicity, as well as protein release process of the novel gel system were investigated.

2. Materials and methods

2.1. Modification of chitosan with 2-iminothiolane hydrochloride

400 mg of chitosan (viscosity: 50–800 mPa s, degree of deacetylation: 80–95%, Sinopham Chemical Reagent Co., Ltd., China) was dissolved in 200 mL 1% acetic acid for 5 h to obtain a 0.2% (w/v) chitosan solution. 40 mg of 2-iminothiolane hydrochloride (Sigma–Aldrich, USA) was added into the chitosan solution and the pH was adjusted to 6 by dropwise addition of 5 M NaOH. After continuous stirring at room temperature for 24 h, the resulting polymer conjugate, chitosan-4-thio-butylamidine (chitosan-TBA), was dialyzed against 5 mM HCl once, 5 mM HCl containing 1% NaCl twice, 5 mM HCl once and finally 1 mM HCl once, 1 day for each time. Finally, the aqueous polymer solution was lyophilized at −50 °C and 20 Pa to obtain the chitosan-TBA sample. The sample should be used immediately for the reason that the thiol groups of chitosan-TBA can be easily oxidized in air.

2.2. Determination of the thiol group content

The thiol group content on chitosan-TBA was determined with Ellman's reagent method described in reference (Bernkop-Schnürch, Hornof, & Zoidl, 2003). Briefly, 5 mg of chitosan-TBA was dissolved in 2.5 mL deionized water. Then, 250 μL of 0.5 M phosphate buffer (pH 8.0) and 500 μL of Ellman's reagent (3 mg of 5,5-dithiobis (2-nitrobenzoic acid) (DTNB) dissolved in 10 mL of 0.5 M phosphate buffer (pH 8.0)) were added. After an incubation period of 2 h at room temperature, the solution was centrifuged at 12,000 rpm for 5 min. Thereafter, 100 μL of the supernatant was transferred into a 96-well plate (Corning, USA) and the absorbance was measured at 450 nm by the microplate reader. A standard curve of known concentrations of L-cysteine hydrochloride was generated concurrently and used to determine the amount of thiol groups.

2.3. Preparation of CS-TBA/HA/β-GP thermo-sensitive hydrogel

200 mg of CS-TBA was dissolved in 9 mL deionized water to obtain a homogeneous solution. 200 mg of nano-hydroxyapatite (HA) powder (obtained from Institute of Nuclear and New Energy Technology, Tsinghua University) was added into the solution with continuous stirring until uniformly distributed. Afterwards, the β-glycerophosphate disodium (β-GP) solution (560 mg of β-GP in 1 mL deionized water) was carefully added into the CS-TBA/HA hybrid drop by drop under constant stirring. The CS-TBA/HA/β-GP hybrid was incubated at 37 °C for several minutes to undergo sol–gel transition. The unmodified chitosan (CS) was used instead of CS-TBA as the control. The CS/HA/β-GP hydrogel was prepared with the same procedure except that the solvent was 0.1 M HCl because chitosan is insoluble in deionized water. The final composition of both CS-TBA/HA/β-GP and CS/HA/β-GP system is 200 mg CS-TBA or CS, 200 mg HA and 560 mg β-GP in 10 mL deionized water (for CS-TBA/HA/β-GP system) or 0.1 M HCl (for CS/HA/β-GP system).

2.4. Scanning electron microscopy (SEM) observation of hydrogel

The CS-TBA/HA/β-GP gel was frozen at −20 °C and lyophilized at -50 °C and 20 Pa for 2 days until all water was sublimed. The freeze-dried sample was surface metalized by sputter-coating with gold for SEM examination. The interior morphology of the hydrogel was observed using SEM (JSM-7001F).

2.5. Structure and composition analysis of hydrogel

The lyophilized sample of CS-TBA/HA/β-GP gel was ground into a powder for the structure and composition analysis. X-ray diffractometer (XRD) was employed for the phase analysis. The data was recorded with the 2θ range from 10° to 70°. X-ray photoelectron spectroscopy (XPS, ESCALAB-250Xi) was employed for the element composition and chemical states analysis using a monochromatic Al Kα X-ray source. For the survey spectra, the pass energy was 100 eV and the energy resolution was 1 eV. For the S2p high resolution spectra, the pass energy was 20 eV and the energy resolution was 0.05 eV. Binding energy is calibrated with C 1s = 284.8 eV.

2.6. Rheological analysis

Rheological measurements were carried out on Physica MCR300 Modular Compact Rheometer (Germany) using a standard steel parallel-plate geometry of 25 mm in diameter. The hydrogel in cylindrical shape (~30 mm in diameter and ~5 mm in height) was placed in the middle between two parallel plates. The shear stress sweep method was employed to test the storage modulus (G') and loss modulus (G'') of the two kinds of hydrogels. All measurements were carried out at a constant temperature (25 °C) and a constant frequency (1 Hz). The shear stress ranged from 1 Pa to 1000 Pa and the G', G'' and complex viscosity (η^*) were recorded.

2.7. In vitro degradation of hydrogel

The CS-TBA/HA/β-GP gel and CS/HA/β-GP gel were both cut into small cubes with a size about 6 mm × 6 mm × 6 mm. Each cube was accurately weighted (w_i) and placed into a well of a 24-well plate. 2 mL of PBS (pH 7.4, containing 25 ppm sodium azide) was added into every well of the 24-well plate. The *in vitro* degradation experiment was conducted at 37 °C under continuous shaking (60 rpm). At designed time intervals, the cubes were sampled and accurately weighted (w_t) after removing the water on the surfaces of the hydrogel with filter paper. A 2-mL aliquot of PBS was replaced by fresh PBS once a week. The weight loss percentage (w%) was used to evaluate degradation of the hydrogels according Eq. (1).

$$w\% = \frac{w_i - w_t}{w_i} \times 100 \quad (1)$$

2.8. In vitro protein release from hydrogel

Bovine serum albumin (BSA) was selected as a model protein to study the protein release process from CS-TBA/HA/β-GP gel or CS/HA/β-GP gel. 0.5 mL CS-TBA/HA/β-GP or CS/HA/β-GP hybrid containing 0.5% (w/v) BSA was placed in a 5-mL Eppendorf tube and incubated at 37 °C to form a gel. Thereafter, 2.5 mL 0.01 M PBS (pH 7.4, containing 25 ppm sodium azide) was added into the

Eppendorf tube. All the samples were incubated at 37 °C under continuous shaking (60 rpm). At designed time intervals, a 1-mL aliquot of the release medium were sampled and replaced with an equal volume of fresh PBS. The concentration of BSA in the release medium was determined with the BCA Assay Kit (Beyotime, China) according to the company's guidelines. The accumulated release amount was calculated according to Eq. (2) (Chen, Dong, Yang, & Deng, 2012).

$$E = \frac{V_E \sum_1^{n-1} C_i + V_0 C_n}{m_0} \times 100\% \quad (2)$$

where E is the accumulated release amount (%); V_E is the sampling volume (1 mL); V_0 is the initial volume (2.5 mL); C_i and C_n are the drug concentrations (μg/mL); i and n are the sampling times; and m_0 is the mass of drug in gel (2500 μg).

2.9. In vitro cytotoxicity of hydrogel

The cytotoxicity of CS-TBA/HA/β-GP gel and CS/HA/β-GP gel extracts were evaluated by Cell Count Kit-8 (CCK-8, Dojindo, Japan) assay using human bone-marrow mesenchymal stem cells (hMSCs) *in vitro*. 0.5 mL of CS-TBA/HA/β-GP or CS/HA/β-GP hybrid was incubated at 37 °C to form a gel. The extract of the gel was prepared by immersing the gel into 10 mL low glucose Dulbecco's modified Eagle's medium (LG-DMEM, Invitrogen, USA). hMSCs were expended in LG-DMEM, containing 10% fetal bovine serum (FBS, Invitrogen, USA), 100 μg/mL streptomycin, 100 U/mL penicillin and used at passage 6. hMSCs (5×10^3 cells/well) were seeded in a 48-well plate and incubated under standard culture condition (5% CO_2, 37 °C) for 24 h. Then the supernatants were placed by the extracts of two kinds of hydrogels. The LG-DMEM without extracts was employed as the control. The supernatants were replaced with fresh medium every 2 days. At day 1, 3 and 5 after seeding, CCK-8 with a 10% vol. of the medium was added into each well and incubated for 3 h at 37 °C. The absorbance (O.D.) of the solution was measured by microplate reader at 450 nm.

2.10. Statistical analysis

Experimental results were expressed as mean ± standard deviation (S.D.). The significance of differences in means was determined using least significant difference (LSD) method.

3. Results and discussion

3.1. Gel formation

The addition of the β-GP solution, a weak base, into the CS-TBA/HA hybrid increased the pH of the system, from 5.4 to 6.8, which is physiologically acceptable (Chenite et al., 2000). The CS-TBA/HA/β-GP system presented a flowing state at room temperature (Fig. 1a). However, the system transformed into a hydrogel after incubated at 37 °C for about 10 min (Fig. 1b). It should be noticed that the precipitation of chitosan occurs at a pH above 6.2 when using a strong base (Huang et al., 2011). The addition of β-GP instead of a strong base can maintain solubility of chitosan probably because of its mild base character and the exposed glycerol moieties to separate chitosan chains in solution at low temperature (Chenite et al., 2001). Upon heating, electrostatic attraction between oppositely charged ammonium groups ($-NH_3^+$) of chitosan and the phosphate moieties of β-GP ($-PO_4^-$) could reduce electrostatic repulsion force, thus induced the attractive hydrophobic and hydrogen bonding between chitosan chains (Chenite et al., 2001; Han et al., 2004; Khodaverdi et al., 2012). The gelation mechanism of CS/β-GP system has been widely reported (Chenite et al., 2001; Han et al., 2004; Khodaverdi et al., 2012). The gelation process of this system depends on pH, temperature, concentration of chitosan and β-GP, and degree of deacetylation (Han et al., 2004; Khodaverdi et al., 2012). By increasing the degree of deacetylation, which is corresponding to the substituted amine groups in CS, the gelation time decreases (Khodaverdi et al., 2012). Furthermore, the gelling temperature decreases at high pH, which suggests that the number of charged ammonium groups in CS is an important parameter controlling gelation in this system (Han et al., 2004). These findings can support the above-mentioned mechanism. For CS-TBA/HA/β-GP system, the thiol groups in CS-TBA, 66.0 ± 0.7 μmol/g determined by Ellman's regent, also contributed to the gel formation due to the formation of inter- and/or intramolecular disulfide bonds. It should be mentioned that this process is not thermosensitive. The formation of disulfide bonds is time-dependent. The sol–gel process of CS-TBA/HA/β-GP is schematically shown in Fig. 1c and d.

3.2. Morphology of CS-TBA/HA/β-GP hydrogel

The nano-hydroxyapatite (HA) powder was added into the solution with continuous stirring until well dispersed at room temperature. After incubation at 37 °C for several minutes, the CS-TBA/HA/β-GP hybrid transformed into an ivory white hydrogel. The interior morphology of the freeze dried CS-TBA/HA/β-GP hydrogel was characterized by SEM, as shown in Fig. 2. The CS-TBA/HA/β-GP hydrogel forms a uniform network because of the crosslinks of chitosan chains. The highly porous structure of CS-TBA/HA/β-GP hydrogel can be clearly observed in Fig. 2a and the average pore size is 40–80 μm. Fig. 2b exhibits the enlarged view of CS-TBA/HA/β-GP hydrogel. The matrix of chitosan network is not smooth but attached by the nano-HA particles. The nano-HA particles are uniformly distributed on the chitosan network. The energy diffraction spectrum (EDS) results confirmed the existence of HA due to the existence of calcium (data not shown). Fig. 2d shows the uniform distribution of Ca element in the area shown in Fig. 2c, it is the evidence for the uniform distribution of HA [$Ca_{10}(PO_4)_6(OH)_2$]. The porous structure of CS-TBA/HA/β-GP hydrogel suggests its potential application in tissue engineering; it can be used as a carrier for drug delivery or as a scaffold for cell infiltration and growth as well (Chen et al., 2012; Shi, Ji, Zhang, Shu, & Wu, 2011).

3.3. Structure and composition analysis of CS-TBA/HA/β-GP hydrogel

The XRD pattern of CS-TBA/HA/β-GP hydrogel is shown in Fig. 3. The standard HA pattern (PDF#09-0432) is also shown at the bottom of this figure. The pure chitosan has a reflection peak at around 20°, indicating its degree of crystallinity (Cui et al., 2011). While after forming a gel, the degree of crystallinity decreased obviously, leaving a weak and broad peak at around 20°, which is mainly because the intermolecular interaction destroyed the regularity of chitosan (Tang, Du, Li, Wang, & Hu, 2009). The other peaks shown in Fig. 3 are all the reflection peaks of HA, which accord with the standard pattern of HA very well, for example, 25.8° for 0 0 2 diffraction, around 32° for overlapping diffractions of 2 1 1 and 1 1 2, 32.9° for 3 0 0 diffraction and 34.1° for 2 0 2 diffraction (Degirmenbasi, Kalyon, & Birinci, 2006). The presence of these peaks suggests that the preparation method has no significant influence on the crystal structure of HA. HA is the most stable and least soluble calcium phosphate compound at normal temperature and the pH 4–12. During the preparation of CS-TBA/HA/β-GP hydrogel, the pH increased from 5.2 to 6.8 and the temperature raised from room temperature to 37 °C, so there is no phase change for HA in this condition.

XPS was employed to analyze the chemical composites and states of CS-TBA/HA/β-GP hydrogel. The survey spectrum is shown

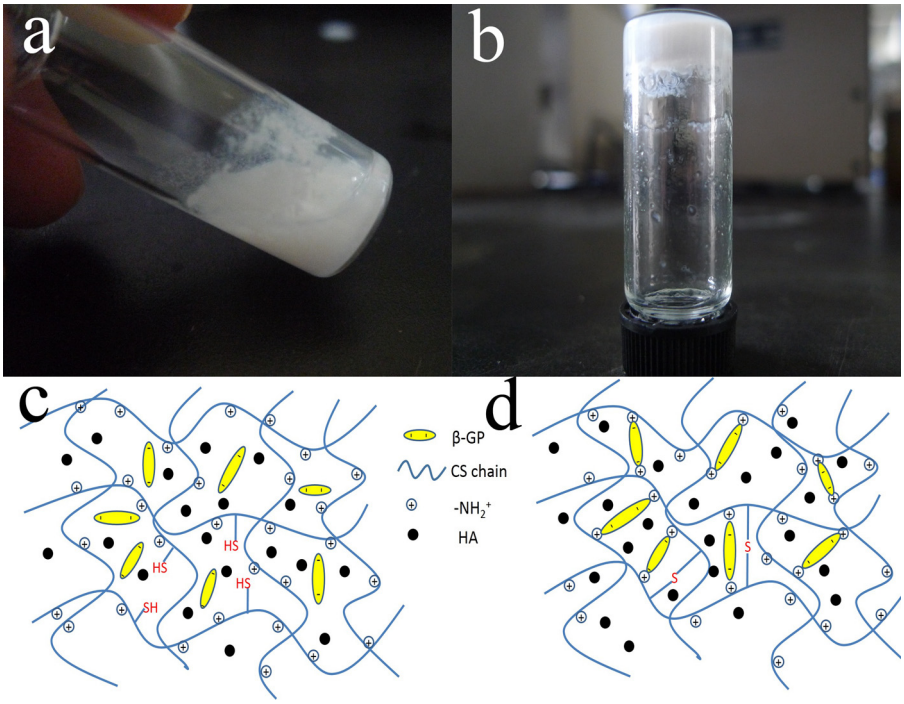

Fig. 1. CS-TBA/HA/β-GP system. (a) CS-TBA/HA/β-GP aqueous solution at room temperature. (b) CS-TBA/HA/β-GP hydrogel at 37 °C. (c) Schematic inner structure of CS-TBA/HA/β-GP aqueous solution at room temperature. (d) Schematic inner structure of CS-TBA/HA/β-GP hydrogel at 37 °C.

in Fig. 4a. The peaks of P2p at 131.6 eV, C1s at 284.8 eV, Ca2p at 345.5 eV, N1s at 398.0 eV, and O1s at 531.0 eV were all detected in the hydrogel. The peak of S2p in the survey spectrum of CS-TBA/HA/β-GP hydrogel is not strong enough, mainly due to the low content of S (only 0.56 at.% determined by XPS). The S2p high resolution XPS spectrum of the hydrogel is shown in Fig. 4b. The S2p spectrum of CS-TBA/HA/β-GP gel has a doublet structure due to the presence of the $S2p_{3/2}$ and $S2p_{1/2}$ peaks (Castner, Hinds, & Grainger, 1996). The spectrum can be fitted using a 2:1 peak area ratio and a 1.2 eV splitting (Vance et al., 2002). The $S2p_{3/2}$ ($S2p_{1/2}$) peaks lie at 161.8 eV (163.0 eV) and 166.8 eV (168.0 eV) imply the presence of two different chemical states of sulfur which can be assigned to free thiol groups and disulfide bonds (Wang et al., 2009).

3.4. Rheology of CS/HA/β-GP and CS-TBA/HA/β-GP hydrogels

The storage modulus (G') and loss modulus (G'') with hydrogels as increasing of oscillatory shear stress of the two kinds of

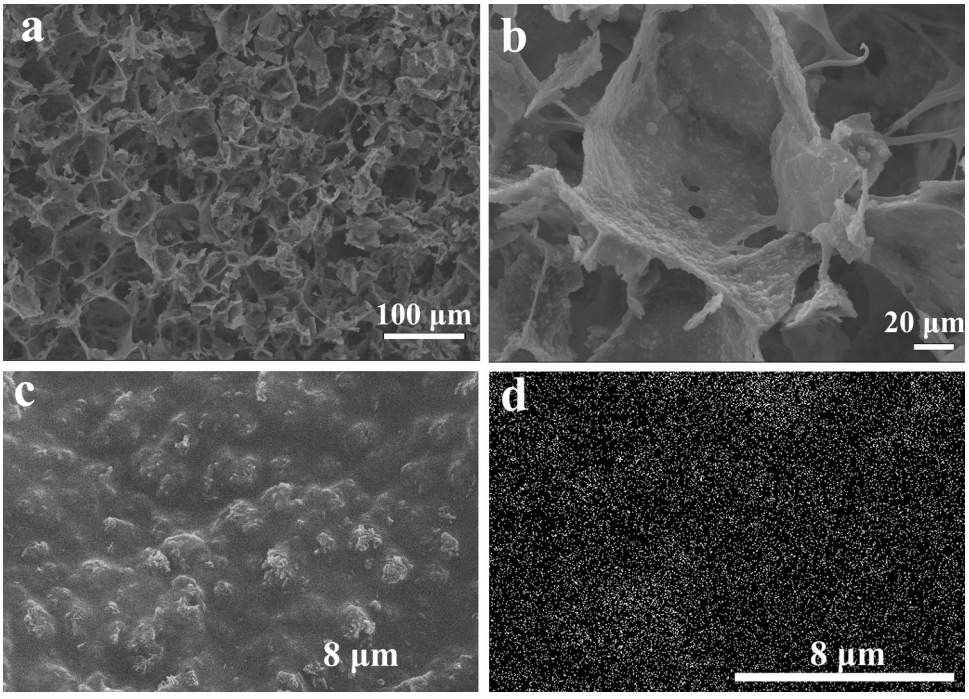

Fig. 2. (a–c) SEM images of lyophilized CS-TBA/HA/β-GP hydrogel. (d) Mapping of Ca element of the area shown in (c).

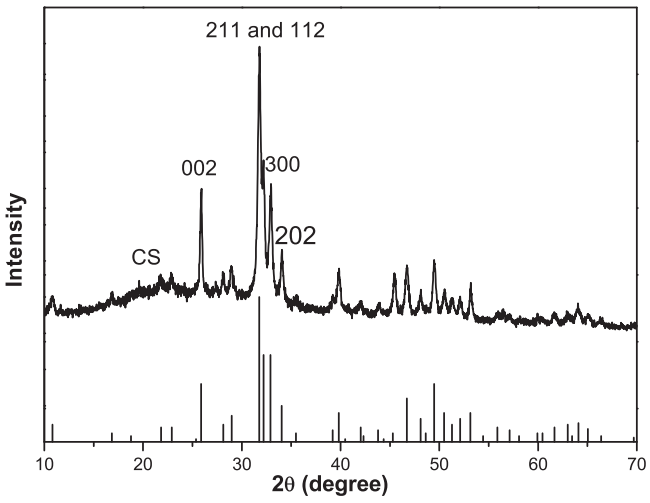

Fig. 3. XRD pattern of lyophilized powder of CS-TBA/HA/β-GP hydrogel. The numbers on the top of peaks are assigned to crystal face indexes of HA. The standard pattern of HA (PDF#09-0432) is also shown in the bottom of the figure.

hydrogels are displayed in Fig. 5a. It can be seen that for each kind of hydrogel, G' is much higher than G'', indicating a typical strong gel (Cho, Heuzey, Bégin, & Carreau, 2006). The G' and G'' of CS/HA/β-GP gel and CS-TBA/HA/β-GP gel are both independent on applied oscillatory shear stress. No obvious decrease is observed between 1 and 1000 Pa, showing that the two kinds of gels both keep their complete structure in this range (Shi et al., 2011; Weng, Chen, & Chen, 2007). While compared with those of CS/HA/β-GP gel, G' and G'' of CS-TBA/HA/β-GP gel are both a little higher. The G' and G'' of CS-TBA/HA/β-GP gel are about 2.0×10^4 Pa and 1.7×10^3 Pa respectively, both are about 1.3 times that of CS/HA/β-GP gel. The significant difference ($p < 0.01$) between the magnitude of complex viscosity (η^*) of the two kinds of gels is shown in Fig. 5b. η^* can be determined according to Eq. (3) (Rao & Cooley, 1994).

$$\eta^* = \frac{G''}{\omega} - i\frac{G'}{\omega} \tag{3}$$

where ω is the angular frequency (2π in this study). Both G' and G'' are positive over the entire temperature range, so that the magnitude of η^* is considered to be a reliable measure of gel strength (Rao & Cooley, 1994). The measured G' or G'' increased with an increase in the intermolecular crosslinks in the hydrogel network (Weng et al., 2007; Wu et al., 2009). For example, increasing the content of free thiol groups in CS-NAC increased the crosslink density, which resulted in an increase of G' (Wu et al., 2009). In our study, for the CS-TBA/HA/β-GP, in addition to the physical crosslink due to β-GP, the chemical crosslink caused by the formation of disulfide bond between two thiol groups enhanced the intermolecular crosslink in the hydrogel network.

3.5. *In vitro degradation of CS/HA/β-GP and CS-TBA/HA/β-GP hydrogels*

The degradation of CS/HA/β-GP and CS-TBA/HA/β-GP hydrogels was evaluated by examining the weight loss in PBS (pH 7.4, containing 25 ppm sodium azide) at 37 °C. As shown in Fig. 6, both kinds of hydrogels show similar degradation behavior in 28 days. There is no significant difference ($p > 0.05$) in the weight loss between two kinds of hydrogels at each designed time. Both kinds of hydrogels degraded relatively rapidly in the first 10 days, probably due to the un-crosslinked β-GP salt in the hydrogels diffusing to the degradation liquid (Chen et al., 2012). Then during the days 10–18, the weight loss of both kinds of hydrogels does not change so much. After 18 days, the degradation rate of both kinds of hydrogels shows a slight increase, which is mainly because of the degradation of chitosan backbone. The degradability of chitosan is mainly controlled by the degree of deacetylation (DD). The low DD chitosan performs high degradation rate because of its low crystallinity (Ganji, Abdekhodaie, & Ramazani, 2007; Zhang & Neau, 2001). At day 21 and 28, the weight loss of both kinds of hydrogels does not increase obviously. The weight loss of CS/HA/β-GP and CS-TBA/HA/β-GP hydrogels after 28 days is $48.58 \pm 2.38\%$ and $51.73 \pm 2.87\%$, respectively. The modification of chitosan does not decrease the degradation rate significantly, even though it increases the crosslink density. This indicates that in CS-TBA/HA/β-GP hydrogel, not only the hydrolysis of disulfide bonds, but also the degradation of chitosan backbone are important in breaking down of the hydrogel (Weng, Romanov, Rooney, & Chen, 2008).

3.6. *In vitro protein release from CS/HA/β-GP and CS-TBA/HA/β-GP hydrogels*

The cumulative release amounts of BSA protein from CS/HA/β-GP and CS-TBA/HA/β-GP hydrogels are shown in Fig. 7. For both kinds of hydrogels, the BSA release behaviors perform similarly. Both have an initial burst effect in the first 2 days, which can be fitted according to zero-order kinetic model ($R^2 = 0.989$ and 0.998

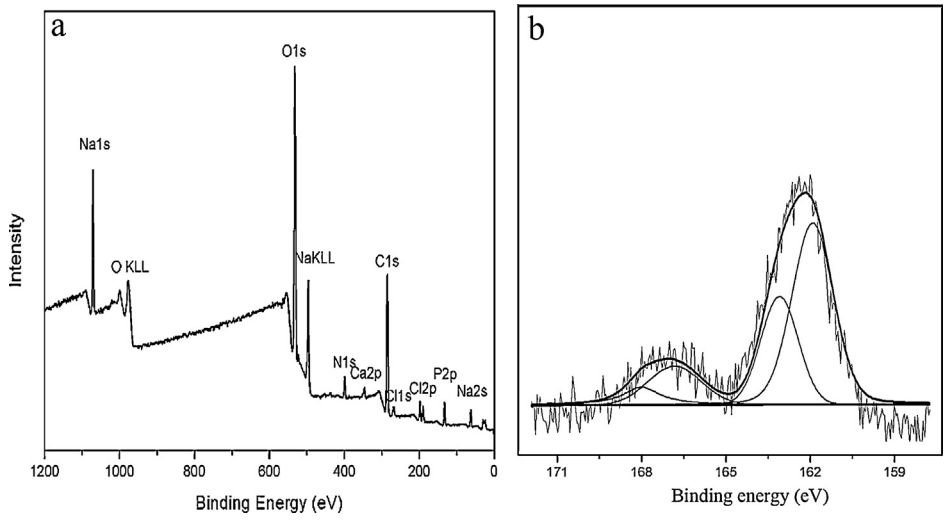

Fig. 4. XPS spectra of lyophilized powder of CS-TBA/HA/β-GP hydrogel. (a) Survey spectrum; (b) High resolution spectrum of S2p.

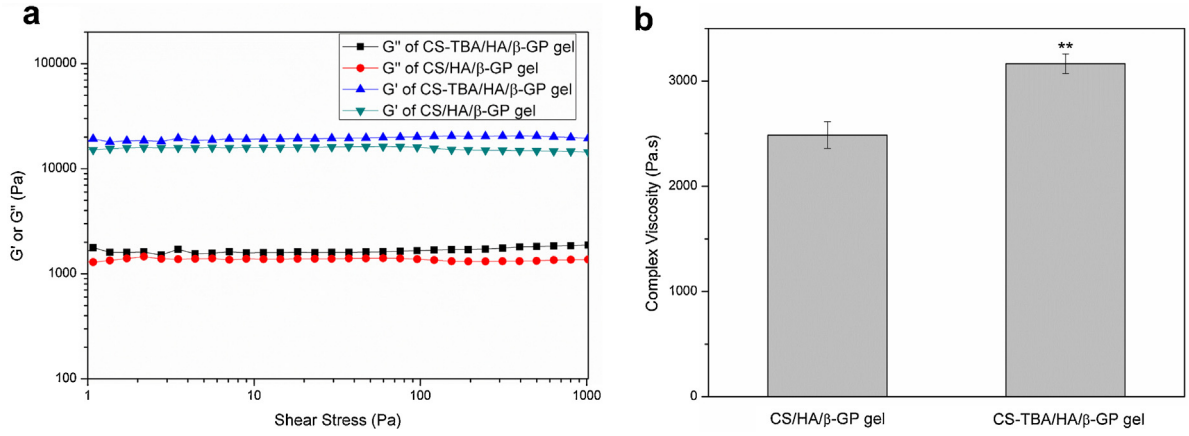

Fig. 5. (a) Dependence of storage modulus (G') and loss modulus (G'') on shear stress for CS/HA/β-GP and CS-TBA/HA/β-GP hydrogels. (b) Complex viscosity (η^*) of CS/HA/β-GP and CS-TBA/HA/β-GP hydrogels.

for CS/HA/β-GP and CS-TBA/HA/β-GP gel, respectively). The initial burst release rates are 39.46% and 32.88% per day for CS/HA/β-GP and CS-TBA/HA/β-GP gel, respectively. The burst release behavior was also observed in the reference, which may be assigned to the immediate dissolution and/or release of the accumulated protein on the surface or in the tunnels of gels during the gelation process (Khodaverdi et al., 2012).

After 2 days, the BSA release rates from both kinds of hydrogels decrease largely. The period of sustained release continued until day 20 for CS-TBA/HA/β-GP gel with a cumulative release of 98.8%. While for CS/HA/β-GP gel, the period of sustained release could maintain until day 12, with a cumulative release of 100%. The release profiles for both kinds of gels are not linear, but more like diffusion-controlled release. Diffusion-controlled release through the hydrogel mesh is the primary mechanism of release of many drugs from hydrogels. BSA has a sustained release due to its relatively large hydrodynamic radius (Bhattarai, Gunn, & Zhang, 2010). Compared with that from CS/HA/β-GP gel, the BSA release from CS-TBA/HA/β-GP gel had a slower rate and maintained a longer time, which can be attributed to the effect of the thiol groups and disulfide bonds. BSA has 36 cysteine residues that form 18 disulfide bonds (Qiu et al., 2003). These disulfide bonds enable BSA to form disulfide-linked covalent aggregates with CS-TBA *via* thiol-disulfide interchange reaction (Ekici, 2011).

Our result can be supported by a previous experiment, in which the release of Insulin from CS/β-GP gel was studied. In their work, the sustained release of Insulin from CS/β-GP gel lasted ~350 h (~288 h in our study for BSA from CS/HA/β-GP gel) (Kempe et al., 2008).

3.7. *In vitro* cytotoxicity of CS/HA/β-GP and CS-TBA/HA/β-GP hydrogels

The cytotoxicity of CS/HA/β-GP and CS-TBA/HA/β-GP hydrogels extracts was measured by CCK-8 method *in vitro* using hMSCs as model cells. CCK-8 can be transformed into orange-colored formazan by the activity of dehydrogenases in cells. The absorbance at 450 nm indicates the number of living cells indirectly. As shown in Fig. 8, after 3 or 5 days' culture, the cell numbers of all three groups increased significantly ($p < 0.01$) compared with those at day 1. There are no significant differences ($p > 0.05$) among the three groups during the cell culture expect at day 1, showing that both CS/HA/β-GP and CS-TBA/HA/β-GP hydrogels extracts have low cytotoxicity *in vitro*. The cytotoxicity of CS-TBA was reported to be concentration-dependent and the concentration of CS-TBA at 0.025% in medium had a negligible cytotoxicity (Guggi, Langoth, Hoffer, Wirth, & Bernkop-Schnürch, 2004). CS-TBA nanoparticles are also considered relatively less toxic for the

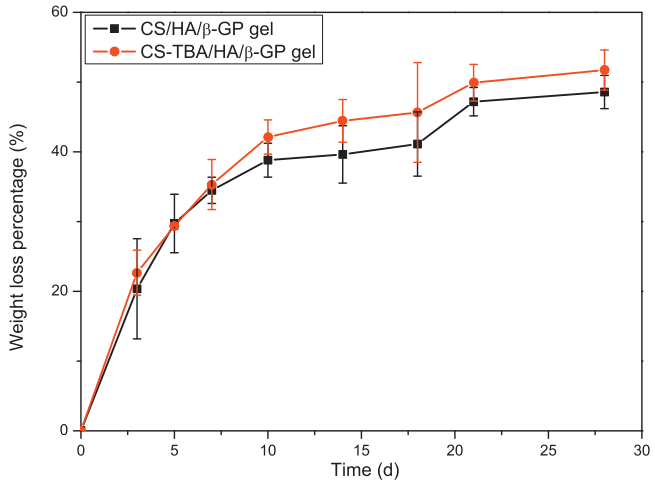

Fig. 6. Degradation profiles of CS/HA/β-GP and CS-TBA/HA/β-GP hydrogels exposed to PBS (pH 7.4) at 37 °C *in vitro*. Data were expressed as means ± SD ($n = 4$ for each sample).

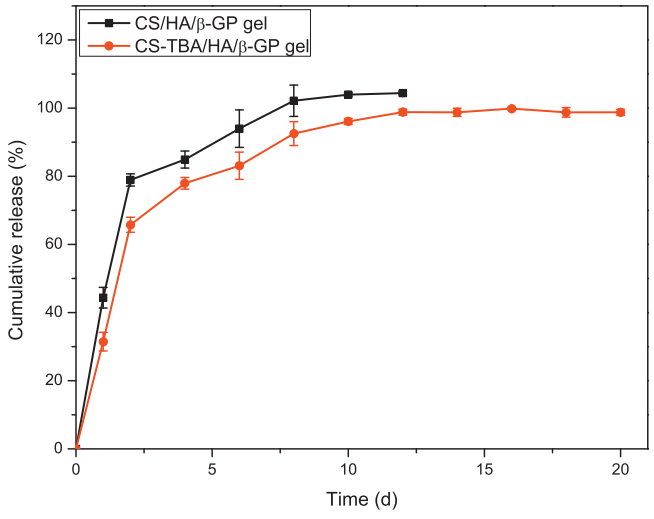

Fig. 7. BSA release profiles from CS/HA/β-GP and CS-TBA/HA/β-GP hydrogels *in vitro*. Data were expressed as means ± SD ($n = 4$ for each sample).

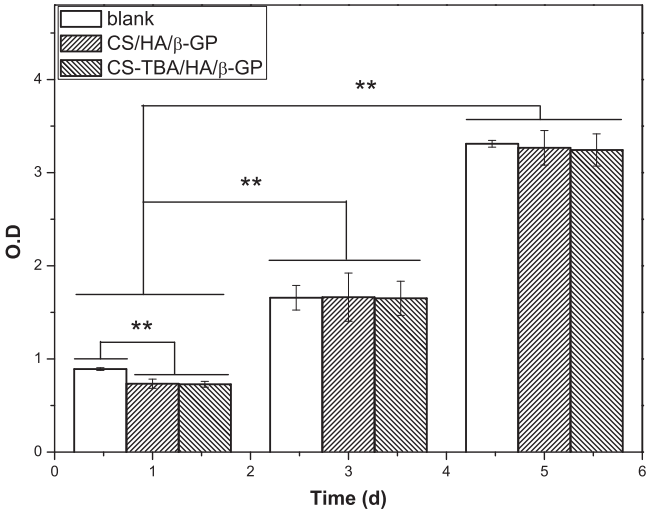

Fig. 8. *In vitro* cytotoxicity of CS/HA/β-GP and CS-TBA/HA/β-GP hydrogels extracts for hMSCs. Data were expressed as means ± SD ($n = 8$ for each sample). Double asterisks (**) denote statistical significance $p < 0.01$.

Caco-2 cells when added into culture medium (Sakloetsakun, Perera, Hombach, Millotti, & Bernkop-Schnürch, 2010). In this study, the CS-TBA/HA/β-GP hydrogel extract exhibited low cytotoxicity for hMSCs *in vitro*, indicating its potential application in biomedicine.

4. Conclusion

In this study, a novel thermo-sensitive hydrogel based on thiolated chitosan, hydroxyapatite and β-glycerophosphate disodium (CS-TBA/HA/β-GP) was prepared. The CS-TBA/HA/β-GP system can form a gel at body temperature. The CS-TBA/HA/β-GP has a higher storage modulus (G') and loss modulus (G''), decreases the BSA release rate and maintains the protein release for a longer time compared with unmodified chitosan system (CS/HA/β-GP), due to the existing thiol groups and/or disulfide bonds. The CS-TBA/HA/β-GP gel has a porous structure with a uniform distribution of nano-hydroxyapatite, an appropriate degradation rate and low cytotoxicity, showing potential applications in drug delivery and tissue engineering.

Acknowledgments

The authors are grateful for the financial support from National Natural Science Foundation of China (51361130032 and 81101348) and Doctor Subject Foundation of the Ministry of Education of China (20120002130002).

References

Bernkop-Schnürch, A., Hornof, M., & Zoidl, T. (2003). Thiolated polymers–thiomers: Synthesis and in vitro evaluation of chitosan-2-iminothiolane conjugates. *International Journal of Pharmaceutics*, *260*(2), 229–237.

Bhattarai, N., Gunn, J., & Zhang, M. (2010). Chitosan-based hydrogels for controlled, localized drug delivery. *Advanced Drug Delivery Reviews*, *62*(1), 83–99.

Castner, D. G., Hinds, K., & Grainger, D. W. (1996). X-ray photoelectron spectroscopy sulfur 2p study of organic thiol and disulfide binding interactions with gold surfaces. *Langmuir*, *12*(21), 5083–5086.

Chen, C., Dong, A., Yang, J., & Deng, L. (2012). Preparation and properties of an injectable thermo-sensitive double crosslinking hydrogel based on thiolated chitosan/beta-glycerophosphate. *Journal of Materials Science*, *47*, 2509–2517.

Chen, X., & Park, H. (2003). Chemical characteristics of O-carboxymethyl chitosans related to the preparation conditions. *Carbohydrate Polymers*, *53*(4), 355–359.

Chenite, A., Buschmann, M., Wang, D., CHAut, C., & Kandani, N. (2001). Rheological characterisation of thermogelling chitosan/glycerol-phosphate solutions. *Carbohydrate Polymers*, *46*(1), 39–47.

Chenite, A., CHAut, C., Wang, D., Combes, C., Buschmann, M. D., Hoemann, C. D., et al. (2000). Novel injectable neutral solutions of chitosan form biodegradable gels in situ. *Biomaterials*, *21*(21), 2155–2161.

Chi, N., Yang, M., Chung, T., Chou, N., & Wang, S. (2013). Cardiac repair using chitosan-hyaluronan/silk fibroin patches in a rat heart model with myocardial infarction. *Carbohydrate Polymers*, *92*(1), 591–597.

Cho, J., Heuzey, M., Bégin, A., & Carreau, P. J. (2006). Viscoelastic properties of chitosan solutions: Effect of concentration and ionic strength. *Journal of Food Engineering*, *74*(4), 500–515.

Cho, M. H., Kim, K. S., Ahn, H. H., Kim, M. S., Kim, S. H., Khang, G., et al. (2008). Chitosan gel as an in situ-forming scaffold for rat bone marrow mesenchymal stem cells in vivo. *Tissue Engineering Part A*, *14*(6), 1099–1108.

Cui, J., Jiang, B., Liang, J., Sun, C., Lan, J., Sun, X., et al. (2011). Preparation and characterization of chitosan/β-GP membranes for guided bone regeneration. *Journal of Wuhan University of Technology – Materials Science Edition*, *26*(2), 241–245.

Degirmenbasi, N., Kalyon, D. M., & Birinci, E. (2006). Biocomposites of nanohydroxyapatite with collagen and poly (vinyl alcohol). *Colloids and Surfaces B: Biointerfaces*, *48*(1), 42–49.

Ekici, S. (2011). Intelligent poly (N-isopropylacrylamide)-carboxymethyl cellulose full interpenetrating polymeric networks for protein adsorption studies. *Journal of Materials Science*, *46*(9), 2843–2850.

Felt, O., Buri, P., & Gurny, R. (1998). Chitosan: A unique polysaccharide for drug delivery. *Drug Development and Industrial Pharmacy*, *24*(11), 979–993.

Frohbergh, M. E., Katsman, A., Botta, G. P., Lazarovici, P., Schauer, C. L., Wegst, U. G. K., et al. (2012). Electrospun hydroxyapatite-containing chitosan nanofibers crosslinked with genipin for bone tissue engineering. *Biomaterials*, *33*(36), 9167–9178.

Ganji, F., Abdekhodaie, M. J., & Ramazani, S. A. A. (2007). Gelation time and degradation rate of chitosan-based injectable hydrogel. *Journal of Sol–Gel Science and Technology*, *42*(1), 47–53.

Guerrero, S., Teijón, C., Muñiz, E., Teijón, J. M., & Blanco, M. D. (2010). Characterization and in vivo evaluation of ketotifen-loaded chitosan microspheres. *Carbohydrate Polymers*, *79*(4), 1006–1013.

Guggi, D., Langoth, N., Hoffer, M. H., Wirth, M., & Bernkop-Schnürch, A. (2004). Comparative evaluation of cytotoxicity of a glucosamine-TBA conjugate and a chitosan-TBA conjugate. *International Journal of Pharmaceutics*, *278*(2), 353–360.

Han, H., Nam, D., Seo, D., Kim, T., Shin, B., & Choi, H. (2004). Preparation and biodegradation of thermosensitive chitosan hydrogel as a function of pH and temperature. *Macromolecular Research*, *12*(5), 507–511.

Hashemi, D., Mirzadeh, H., Imani, M., & Samadi, N. (2013). Chitosan/polyethylene glycol fumarate blend film: Physical and antibacterial properties. *Carbohydrate Polymers*, *92*(1), 48–56.

Huang, Z., Yu, B., Feng, Q., Li, S., Chen, Y., & Luo, L. (2011). In situ-forming chitosan/nano-hydroxyapatite/collagen gel for the delivery of bone marrow mesenchymal stem cells. *Carbohydrate Polymers*, *85*(1), 261–267.

Kafedjiiski, K., Krauland, A. H., Hoffer, M. H., & Bernkop-Schnuech, A. (2005). Synthesis and in vitro evaluation of a novel thiolated chitosan. *Biomaterials*, *26*(7), 819–826.

Kean, T., Roth, S., & Thanou, M. (2005). Trimethylated chitosans as non-viral gene delivery vectors: Cytotoxicity and transfection efficiency. *Journal of Controlled Release*, *103*(3), 643–653.

Kempe, S., Metz, H., Bastrop, M., Hvilsom, A., Contri, R. V., & Mäder, K. (2008). Characterization of thermosensitive chitosan-based hydrogels by rheology and electron paramagnetic resonance spectroscopy. *European Journal of Pharmaceutics and Biopharmaceutics*, *68*(1), 26–33.

Khodaverdi, E., Tafaghodi, M., Ganji, F., Abnoos, K., & Naghizadeh, H. (2012). In vitro insulin release from thermosensitive chitosan hydrogel. *AAPS PharmSciTech*, *13*(2), 460–466.

Kim, T., Jiang, H., Jere, D., Park, I., Cho, M., Nah, J., et al. (2007). Chemical modification of chitosan as a gene carrier in vitro and in vivo. *Progress in Polymer Science*, *32*(7), 726–753.

Kwon, J. S., Kim, G. H., Kim, D. Y., Yoon, S. M., Seo, H. W., Kim, J. H., et al. (2012). Chitosan-based hydrogels to induce neuronal differentiation of rat muscle-derived stem cells. *International Journal of Biological Macromolecules*, *51*(5), 974–979.

Matsuda, A., Kobayashi, H., Itoh, S., Kataoka, K., & Tanaka, J. (2005). Immobilization of laminin peptide in molecularly aligned chitosan by covalent bonding. *Biomaterials*, *26*(15), 2273–2279.

Niu, X., Feng, Q., Wang, M., Guo, X., & Zheng, Q. (2009). Porous nano-HA/collagen/PLLA scaffold containing chitosan microspheres for controlled delivery of synthetic peptide derived from BMP-2. *Journal of Controlled Release*, *134*(2), 111–117.

Qiu, B., Stefanos, S., Ma, J., Lalloo, A., Perry, B. A., Leibowitz, M. J., et al. (2003). A hydrogel prepared by in situ cross-linking of a thiol-containing poly (ethylene glycol)-based copolymer: A new biomaterial for protein drug delivery. *Biomaterials*, *24*(1), 11–18.

Rao, M. A., & Cooley, H. J. (1994). Influence of glucose and fructose on high-methoxyl pectin gel strength and structure development. *Journal of Food Quality*, *17*(1), 21–31.

Sakloetsakun, D., Perera, G., Hombach, J., Millotti, G., & Bernkop-Schnürch, A. (2010). The impact of vehicles on the mucoadhesive properties of orally administrated nanoparticles: A case study with chitosan-4-thiobutylamidine conjugate. *AAPS PharmSciTech*, *11*(3), 1185–1192.

Sarti, F., & Bernkop-Schnuerch, A. (2011). Chitosan and thiolated chitosan. *Advances in Polymer Science*, *243*, 93–110.

Shi, W., Ji, Y., Zhang, X., Shu, S., & Wu, Z. (2011). Characterization of ph- and thermosensitive hydrogel as a vehicle for controlled protein delivery. *Journal of Pharmaceutical Sciences*, *100*(3), 886–895.

Tan, H., Chu, C. R., Payne, K. A., & Marra, K. G. (2009). Injectable in situ forming biodegradable chitosan-hyaluronic acid based hydrogels for cartilage tissue engineering. *Biomaterials*, *30*(13), 2499–2506.

Tang, Y., Du, Y., Li, Y., Wang, X., & Hu, X. (2009). A thermosensitive chitosan/poly (vinyl alcohol) hydrogel containing hydroxyapatite for protein delivery. *Journal of Biomedical Materials Research Part A*, *91A*(4), 953–963.

Vance, A. L., Willey, T. M., van Buuren, T., Nelson, A. J., Bostedt, C., Fox, G. A., et al. (2002). XAS and XPS characterization of a surface-attached rotaxane. *Nano Letters*, *3*(1), 81–84.

Wang, X., Zheng, C., Wu, Z., Teng, D., Zhang, X., Wang, Z., et al. (2009). Chitosan-NAC nanoparticles as a vehicle for nasal absorption enhancement of insulin. *Journal of Biomedical Materials Research Part B: Applied Biomaterials*, *88B*(1), 150–161.

Weng, L., Chen, X., & Chen, W. (2007). Rheological characterization of in situ crosslinkable hydrogels formulated from oxidized dextran and n-carboxyethyl chitosan. *Biomacromolecules*, *8*(4), 1109–1115.

Weng, L., Romanov, A., Rooney, J., & Chen, W. (2008). Non-cytotoxic, in situ gelable hydrogels composed of N-carboxyethyl chitosan and oxidized dextran. *Biomaterials*, *29*(29), 3905–3913.

Wong, K., Sun, G., Zhang, X., Dai, H., Liu, Y., He, C., et al. (2006). PEI-g-chitosan, a novel gene delivery system with transfection efficiency comparable to polyethylenimine in vitro and after liver administration in vivo. *Bioconjugate Chemistry*, *17*(1), 152–158.

Wu, Z. M., Zhang, X. G., Zheng, C., Li, C. X., Zhang, S. M., Dong, R. N., et al. (2009). Disulfide-crosslinked chitosan hydrogel for cell viability and controlled protein release. *European Journal of Pharmaceutical Sciences*, *37*(3–4), 198–206.

Zhang, H., & Neau, S. H. (2001). In vitro degradation of chitosan by a commercial enzyme preparation: Effect of molecular weight and degree of deacetylation. *Biomaterials*, *22*(12), 1653–1658.